

Control of Supercritical Organic Rankine Cycle based Waste Heat Recovery System using Conventional and Fuzzy Self-Tuned PID Controllers

Jahedul Islam Chowdhury, David Thornhill, Payam Soulatiantork, Yukun Hu, Nazmiye Balta-Ozkan, Liz Varga and Bao Kha Nguyen*

Abstract: This research develops a supercritical organic Rankine cycle (ORC) based waste heat recovery (WHR) system for control system simulation. In supercritical ORC-WHR systems, the evaporator is a main contributor to the thermal inertia of the system, which is greatly affected by transient heat sources during operation. In order to capture the thermal inertia of the system and reduce the computation time in the simulation process, a fuzzy-based dynamic evaporator model was developed and integrated with other component models to provide a complete dynamic ORC-WHR model. This paper presents two control strategies for the ORC-WHR system: evaporator temperature control and expander output control, and two control algorithms: a conventional PID controller and a fuzzy-based self-tuning PID controller. The performances of the proposed controllers are tested for set point tracking and disturbance rejection ability in the presence of steady and transient thermal input conditions. The robustness of the proposed controllers is investigated with respect to various operating conditions. The results show that the fuzzy self-tuning PID controller outperformed the conventional PID controller in terms of set point tracking and disturbance rejection ability at all conditions encountered in the paper.

Keywords: Control algorithms, fuzzy logic, organic Rankine cycle, PID controller, supercritical condition, waste heat recovery

1. INTRODUCTION

Over the past few decades global emissions have doubled, with the top three energy-consuming sectors (energy supply sector: 25%, industry: 21% and transport: 14%) accounting for 60% of total emissions [1]. Due to its limited conversion efficiency, a large amount of energy generated by burning of fossil fuels is released into the environment as waste heat, therefore it is very important to recover any waste heat to enhance the conversion efficiency and minimise the environmental impacts. Waste heat from energy-intensive sectors is mostly low (<230°C) and medium (230-650°C) grade of energy [2]. One of the promising waste heat recovery (WHR) technologies for low to medium grade heat is the Organic Rankine cycle (ORC), which can convert waste heat into electricity that avoids the equivalent conversion from other sources.

The ORC is a thermodynamic power cycle consisting mainly of thermo-mechanical devices such as an

evaporator, a pump, a condenser and an expander, as shown in Fig. 1(a). The ORC uses organic fluids instead of water, which is common in the traditional steam Rankine cycle (SRC). The traditional SRC for low and medium grade heat recovery applications is normally designed and operated at a pressure lower than the critical pressure of water, which is called a subcritical cycle; whereas the ORC for similar applications can work not only under subcritical conditions, but also under supercritical conditions - this indicates that the working pressure of the cycle is higher than the critical pressure of the organic fluid (see Fig. 1(b) and (c)).

The basic principle of the supercritical cycle is the same as the subcritical ORC, except that the working fluid is heated up (points 2-3 in Fig. 1(c)) directly in the supercritical state without going through a two-phase state [3]. This heating condition gives a good thermal match between the heat source and the working fluids, thereby improving heat recovery [4]. In recent years, the supercritical ORC has attracted a lot of attention as many

Manuscript received ; revised ; accepted May . Recommended by Associate Editor Soon-Shin Lee under the direction of Editor Milton John. This journal was supported by the Engineering and Physical Sciences Research Council (EPSRC, EP/P004636/1, UK).

Jahedul Islam Chowdhury, Nazmiye Balta-Ozkan are with the School Water, Energy and Environment, Cranfield University, Bedford, MK43 0AL, UK (e-mails: {J.Chowdhury, N.Ozkan}@cranfield.ac.uk), Yukun Hu and Liz Varga are with the Department of Civil, Environmental and Geomatic Engineering, University College London, London, WC1E 6BT, UK (e-mails: {Yukun.Hu, L.Varga}@ucl.ac.uk), David Thornhill is with the school of Mechanical and Aerospace Engineering, Queens University Belfast, BT9 5AH, UK, (e-mail: D.Thornhill@qub.ac.uk), Payam Soulatiantork is with the Department of Automatic Control and Systems Engineering, University of Sheffield, S1 3JD, UK (e-mail: P.Soulatiantork@sheffield.ac.uk), Bao Kha Nguyen is with the School of Engineering and Informatics, University of Sussex, Brighton, BN1 9QT, UK, (e-mail: b.k.nguyen@sussex.ac.uk).

* Corresponding author.

publications can be found on working fluid selection [5], circuit configuration and design [6] and performance analysis and optimisation [3,7–11]. However, most analyses were based on steady-state conditions only, with a limited number of publications on dynamic conditions. Therefore, this paper briefly presents the development of a dynamic supercritical model of the ORC-WHR system, focusing on the evaporator, which is the most crucial contributor to the thermal inertia of the system. Traditionally, evaporator models have always been developed using finite volume (FV) method which has a higher accuracy and can capture the thermal inertia of a system effectively [7,12]. However, due to a numerical approach, the FV method is highly time consuming in simulations and real time applications [7, 13,14]. Therefore, the proposed evaporator model based on fuzzy logic was developed in this research to save computation time and make it suitable for real-time applications.

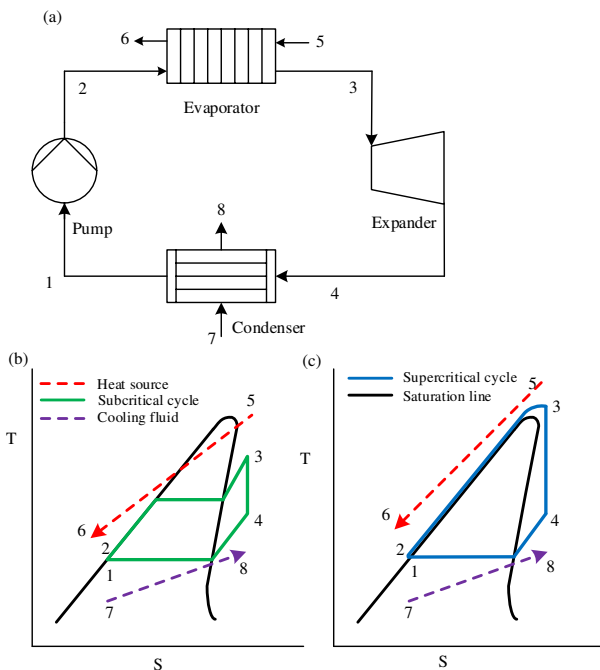


Fig. 1. (a) Schematic diagram of organic Rankine cycle (ORC), (b) T-S (Temperature-Entropy) diagram of Subcritical ORC and (c) Supercritical ORC

The control in real-time ORC systems is always challenging because it has to deal with the dynamic conditions of the heat source, which has many constraints and uncertainties that must be taken into account in control system simulations [15]. To address these challenges, different control strategies such as conventional PID and advanced controllers, e.g. Model Predictive Controllers (MPC), were used for the control of ORC in automobile and power plants [16, 17]. Yebe et al. [17] used a parallel heat exchanger ORC-WHR system for the diesel engine and designed a nonlinear model predictive controller (NMPC) to regulate the output temperatures of both heat exchangers. The controller was then compared to a conventional PID controller and the results showed that the NMPC has less control response time and overshoot. Quoilin et al. [18]

used two PI controllers in the simulation of optimised control strategies for small scale ORC. However, these studies are limited to subcritical ORCs only. Since the research of supercritical ORC is recent and growing, and there is no known control related work in the literature, this paper therefore contributes to the knowledge of existing ORC technology by developing control strategies, e.g. evaporator temperature and expander output controls, and control algorithms for slow response and high thermal inertia WHR system. In this paper, the novel fuzzy based dynamic evaporator model is integrated with other components of the ORC-WHR system, and then uses it for control system simulation. Due to inherent transient nature of waste heat from automotive vehicles and uncertain nonlinearities, the control of supercritical ORC is much more challenging and complex. To address such nonlinearities, fuzzy technique is used to design self-adapting controllers, as proposed in several studies [19,20]. A fuzzy self-tuning PID controller is proposed to control evaporator outlet temperature of the ORC, and to improve the control performance of the conventional PID controller in this research. Another PI controller is added to control the expander output. The performance of both controllers is then investigated and evaluated in this paper.

The rest of the paper is organised as follows. The system dynamic model of the ORC is presented in Section 2. Control problems and strategies are outlined in Section 3. Control simulations for evaporator outlet temperature and expander output are presented and described in Section 4 and 5, respectively. Conclusions and recommendations for future work are provided in Section 6.

2. DYNAMIC MODEL OF WASTE HEAT RECOVERY SYSTEM

Fig. 2 represents a dual-loop WHR system, which consists of a primary ORC loop and a secondary heat transfer loop. The dynamic model of the supercritical ORC-WHR system comprises of a pump, an evaporator, an expander, a condenser, an accumulator, and a valve, as shown in Fig. 2. The heat source fluid is considered to

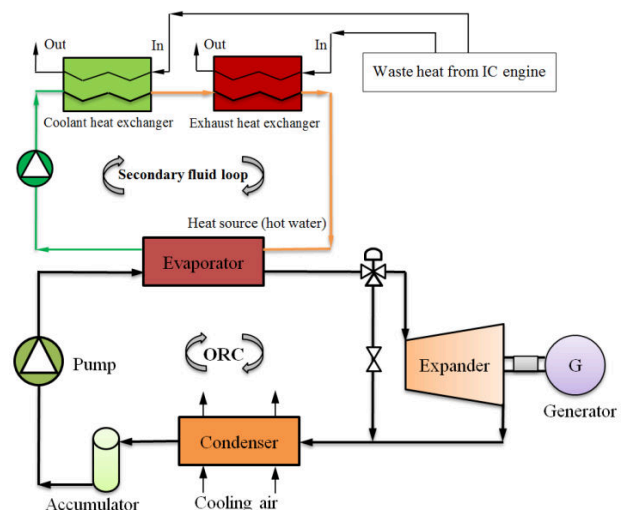


Fig. 2. Dynamic model of ORC-based WHR system.

be waste heat in the form of hot water obtained from an IC engine via the secondary heat transfer loop. This heat source could also be from other applications such as solar plants, steam power plants, geothermal plants, etc. On the other hand, R134a is used as the working fluid of the ORC. Due to the importance of control and energy conversion in the ORC loop, component modelling on the secondary loop in Fig. 2 is ignored.

2.1 Evaporator model

In this work, a plate heat exchanger is chosen as the evaporator. Due to high transient heat sources and the variable thermo-physical properties of a working fluid under supercritical conditions, dynamic models of evaporators are commonly developed using finite volume method [21]. This method is robust and has a higher accuracy than other conventional methods such as zone modelling method. However, the method is extremely time consuming for simulation and cannot be used in real time control applications [7,22]. A novel model of the evaporator using fuzzy logic technique is therefore developed in this paper. The fuzzy logic concept with a time delay can be used to develop a model of a nonlinear system which does not require a set of complex mathematical equations as shown in [23,24]. It requires less resource and saves substantial computation time.

2.1.1 Design of fuzzy based model

The fuzzy based dynamic evaporator model is developed with three inputs and two outputs and consists of two functioning parts: a fuzzy inference system and a thermal inertia block (see Fig. 3). The inputs of the fuzzy model are the refrigerant mass flow rate \dot{m}_r , heat source mass flow rate \dot{m}_h and heat source temperature T_h while the outputs are the evaporator outlet temperature T_{ro} and heat source outlet temperature T_{ho} . For a given set of inputs, the fuzzy inference system calculates T_{r-o} and T_{h-o} , a set of interim crisp values of the final outputs, and feeds the values to the thermal inertia block that accomplishes the inertia part of the model and provides the dynamic model outputs, T_{ro} and T_{ho} .

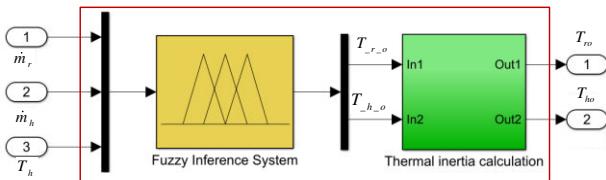


Fig. 3. Fuzzy based dynamic evaporator model

The fuzzy based evaporator model was designed to a specific application and the initial designed parameters were obtained from a robust FV model presented by the authors in [21]. The ranges of the inputs and outputs parameters of the fuzzy model are shown in Table 1. These ranges were determined and adjusted from the experience about the system of the designer. The input and output ranges defined for the fuzzy based model are

classified into different linguistic levels, which are called membership functions. There are six linguistic levels that are used to define the model: VL- Very Low; L- Low; M- Medium; MH- Medium to High, H- High, and VH- Very High. Each of the inputs has three membership functions, while the output T_{ro} has five and T_{ho} has six. The numbers of the membership functions were selected in a way so that they are adequate to represent the nonlinearity of the evaporator and can achieve at least 90% accuracy against the reference FV based evaporator model in [21]. The range of the membership functions and their design can be found in detail in [22].

A permutation of the inputs variables and their membership functions provides a total of 27 fuzzy rules (see Ref. [22]). The fuzzy rules establish the logical relationship between the input variables in space to the output variables. The rules of the fuzzy model are generally defined from the knowledge of characteristics of the system. In this dynamic model, the rules were established from the intuition and knowledge of the evaporator used in this paper.

Table 1. Details of membership functions used in fuzzy model

Variables	Minimum value	Maximum value	Membership function
Mass flow rate of refrigerant, \dot{m}_r	0.01 kg/s	0.25 kg/s	L, M, H
Mass flow rate of heat source, \dot{m}_h	0.05 kg/s	0.30 kg/s	
Temperature of heat source, T_h	400 K	523 K	
Evaporator outlet temperature, T_{ro}	364.5 K	470 K	VL, L, M, H, VH
Heat source outlet temperature, T_{ho}	285 K	595 K	VL, L, M, MH, H, VH

The thermal inertia block, which is the second part of the fuzzy model, calculates the inertial effect based on the geometry and material properties of the evaporator, fluids' flow rates, temperatures and thermo-physical properties of the fluids in the evaporator. The thermal inertia of the model is defined according to the adjustment made from the knowledge of the transient behaviour of the evaporator used in [21], which can be found in [22].

2.1.2 Model validation

In order to validate the fuzzy based dynamic evaporator model, the outputs of the model are compared with that of the renowned finite volume model in [21] and shown in Fig. 4. This figure illustrates that the transient variations of the fuzzy model's outputs are similar with that of the FV model, except small discrepancies in some times in the test period. The goodness of fit, RMSE and MAPE of the fuzzy based model were calculated against the reference data shown in [21]. The fitness, RMSE and MAPE obtained for T_{ro} are at 90.32%, 1.10K, 0.19% and for T_{ho} are at 91.24%, 3.09K, 0.58%, respectively. In addition to these promising numbers, the actual time used for the simulation of the fuzzy based evaporator model was 5.19 s, compared to 3820.6 s for the FV model. That means

the fuzzy model is hundreds of times faster for computation than the FV model. These performance indicator numbers illustrate that the fuzzy logic concept can be utilised to develop the evaporator model for the supercritical ORC-WHR system.

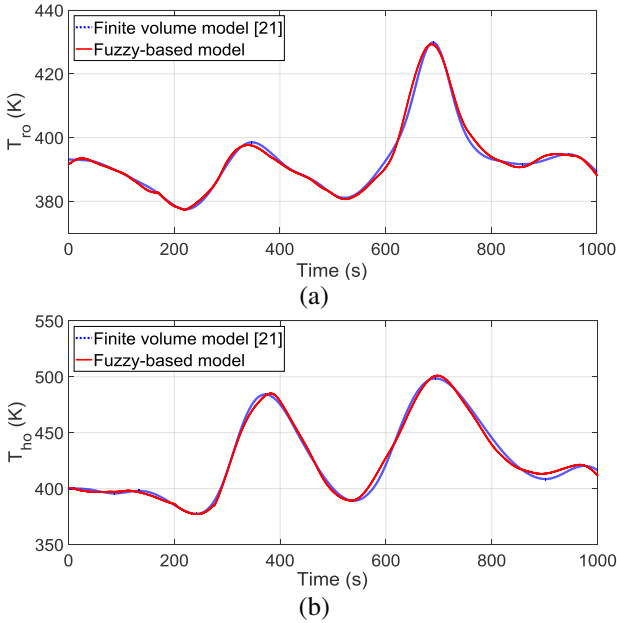


Fig. 4. Comparison of fuzzy and FV based evaporator models outputs, (a) for T_{ro} : Fitness= 90.32%, RMSE= 1.10K, MAPE=0.19% (b) for T_{ho} : Fitness= 91.24%, RMSE= 3.09K, MAPE=0.58%

2.2 Pump and expander models

Since the pump and expander are positive displacement machines, their response time in the operation of the ORC-WHR system is much faster than that of the evaporator. In such a case, complex dynamic models of the pump and expander are unnecessary, and steady state models are sufficient to serve the purpose. The pump used in this research was a diaphragm type, whose mass flow rate is proportional to the speed of the pump [25], while the expander is a scroll type whose model is represented by thermodynamic state enthalpies.

The pump work input W_p is given by

$$W_p = \frac{\dot{m}_p \bar{v}_p (P_{p,o} - P_{p,i})}{\eta_p} \quad (1)$$

The expander work output W_{exp} is given by

$$W_{exp} = \dot{m}_{exp} \eta_{exp} (H_{exp,i} - H_{exp,o}) \quad (2)$$

where \dot{m}_p is the mass flow rate of the pump in kg/s; \bar{v}_p is the average specific volume of the refrigerant in m^3/kg ; $P_{p,i}$ and $P_{p,o}$ are the inlet and outlet pressures of the pump in kPa, respectively. \dot{m}_{exp} is the refrigerant

mass flow rate through the expander; $H_{exp,i}$ and $H_{exp,o}$ are the enthalpy at the inlet and outlet of the expander in kJ/kg, respectively; η_p and η_{exp} are the efficiency of the pump and expander, respectively.

2.3 Condenser and accumulator models

Since dynamic model of the evaporator is of greater importance due to more transient disturbances from a heat source than that of a condenser, the condenser used in this paper is modelled thermodynamically in (3). The accumulator, on the other hand, is represented by a set of time dependent equations. The purpose of the accumulator is to absorb the working fluid fluctuations in the cycle and ensure that there is liquid refrigerant at the inlet of the pump.

The condenser model is given by

$$Q_{con} = \dot{m}_{con} (H_{exp,o} - H_{con,o}) \quad (3)$$

The accumulator model is given by

$$\frac{d\psi}{dt} = \frac{v_{r,l} (\dot{m}_{r,ac,i} - \dot{m}_{r,ac,o})}{V_{ac}} \quad (4)$$

$$\frac{dH_{ac}}{dt} = \frac{\dot{m}_{r,ac,o} v_{r,l} (H_{ac,i} - H_{ac,o})}{V_{ac}} \quad (5)$$

where Q_{con} is the condenser power; ψ is the relative liquid level at the accumulator; $v_{r,l}$ is the specific volume of the refrigerant at liquid state; V_{ac} is the total volume of the accumulator.

2.4 Valve model

The control valve in the WHR system is used to pass a required amount of flow through the expander and the rest of the flow through a by-pass valve as shown in Fig. 5. The modulation between the port A and B can be made using the degree of valve opening of the ports.

The mass flow rate through the valve $\dot{m}_{r,v}$ can be calculated as follows:

$$\dot{m}_{r,v} = \theta A_v \sqrt{2\rho\Delta P} \quad (6)$$

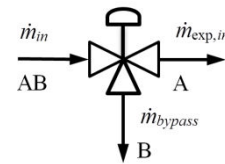


Fig. 5. Three-ways modulating control valve

The pressure loss ΔP in the ORC-WHR system is modelled using the Darcy–Weisbach pressure drop correlation, while the friction factor f_D is estimated by Haaland's correlation [26] as follows:

$$\Delta P_{pipe} = \frac{f_D \rho L_p v^2}{2D_h} \quad (7)$$

$$\frac{1}{\sqrt{f_D}} = -1.8 \log \left[\left(\frac{\epsilon_p / D}{3.7} \right)^{1.11} + \frac{6.9}{Re} \right] \quad (8)$$

where θ is the valve opening (%), A_v is the cross-sectional area in m^2 , ρ is the density of the fluid in kg/m^3 , ΔP is the pressure drop across the valve in kPa, L_p is the length of the pipe in m, v is the velocity of the fluid in m/s, D_h is the hydraulic diameter of the pipe in m. ϵ_p and ϵ_p / D are the absolute and relative roughness of the pipe in m, respectively.

Table 2. ORC model parameters.

Name	Value	Ref.
Evaporator heat transfer area, A	5.78m ²	[21]
Evaporator plate length, L	0.478m	
Evaporator plate width, W	0.124m	
Number of plates, N_{pt}	100	
Thermal conductivity, K	15W/m K	
Pump efficiency, η_p	0.75	
Expander efficiency, η_{exp}	0.8	[27]
Evaporator pressure, P_{ev}	6000 kPa	Assumed
Condenser pressure, P_{con}	770 kPa	Assumed
Condenser temperature, T_{con}	303K	Assumed

Although the steady state model of the pump and the valve are integrated in the dynamic model of the ORC-WHR system, using the models in this form in a control system may lead to unsteadiness and rapid oscillations [18]. To reduce the possible rapid oscillations, the response of the pump speed and the valve are filtered by first-order low pass filters as follows:

$$N_{p_f} = \frac{1}{\tau_p \cdot s + 1} \quad (9)$$

$$g_f = \frac{1}{\tau_v \cdot s + 1} \quad (10)$$

where N_{p_f} is the filter for the pump, g_f is the filter for the valve; τ_p and τ_v are the time constants for the pump and the valve which are assumed to be 2 s and 1 s, respectively.

The values of the time constants represent the actuation delay of the pump and valve which are reasonable as can be seen in the literature [18]. The overall ORC parameters used in the integrated model are shown in Table 2.

3. CONTROL PROBLEMS AND STRATEGIES

Keeping the ORC-WHR system within nominal operating ranges with transient heat sources is always challenging. If the process variables such as evaporator outlet temperature operate beyond the nominal range,

this can be harmful to the system components and affect the performance. The evaporator temperature is therefore a critical parameter that must be controlled during the operation. The temperature should not be too low so as to create liquid droplets when expanding in the expander, yet not too high so that the ORC's components are damaged. Also, it is reported that a higher evaporator temperature is not ideal to achieve greater heat recovery efficiency [18]. Therefore, an ideal temperature of 405 K for R134a was derived from the steady-state analysis of the system and is illustrated in Fig. 6. This temperature meets both the safety requirements and provides reasonable heat recovery efficiency. Also, the selected temperature is the minimum temperature that could prevent the formation of droplets in the expander, which corresponds to the evaporator working pressure of 6000 kPa and an entropy of 1.7 kJ/kg K.

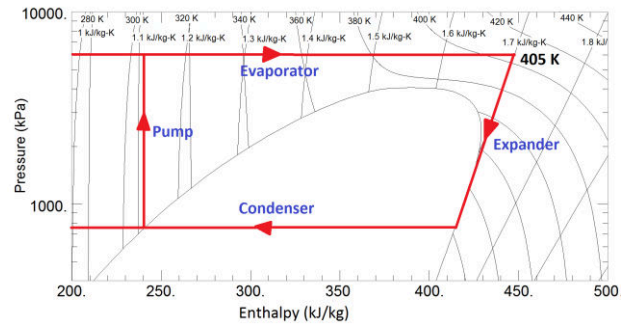


Fig. 6. Selection of evaporator outlet temperature from P-h diagram of R134a

The expander work output in the dynamic model is also affected by the transient heat sources. A sudden variation in the inlet conditions and therefore the output power, can lead to certain critical conditions (i.e. breakdown, hammering, excess wear, etc.) of the expander. Since an expander, in a small-scale WHR system, is an expensive device, the expander power output should be controlled to avoid such unexpected conditions.

In order to keep the operating parameters within a desired operating range and avoid critical conditions, two control strategies are suggested: (1) control of evaporator outlet temperature and (2) simultaneous control of evaporator outlet temperature and expander output.

3.1 Evaporator temperature control

In the first strategy, the evaporator outlet temperature is controlled by the pump of the ORC. In the case of a diaphragm pump, the mass flow rate of refrigerant is dependent on the pump speed. Also, the relationship between the refrigerant mass flow rate and the outlet temperature of the evaporator is such that a modification of the mass flow rate changes the evaporator outlet temperature [18]. Therefore, the pump speed, which regulates the mass flow rate, can be used to control the evaporator outlet temperature. In this control strategy, the evaporator temperature is controlled alone, while the expander is allowed to rotate freely. This strategy is particularly valid in small-scale WHR systems where the expander output is expected to be low and controlling the output may not be beneficial for conversion efficiency of

the cycle.

3.2 Evaporator temperature and expander output control

In the second strategy, the evaporator temperature is controlled by the pump, which is the first strategy, while simultaneously the expander output is proposed to be controlled by the proportional valve used in the ORC. Since the expander work output is a function of the mass flow rate of the refrigerant, control of the valve opening can be used to regulate the work output. Unlike the first strategy, the expander output cannot be controlled alone due to the fact that without the temperature control first, the expander may receive liquid-vapour mixtures and cause damage to it. To control the temperature first, a controller regulates the mass flow rate of the refrigerant which can cause a sudden change of expander power output due to a large control input at any given time. Therefore, the objective of the control of the expander work output is not only to maintain the operation at a predefined set point but also to reduce the sudden rise of the power output.

4. SIMULATION OF EVAPORATOR TEMPERATURE CONTROL

4.1 Conventional PID controller

A conventional single-input-single-output (SISO) parallel type Proportional – Integral – Derivative (PID) controller combined with a first order filter is initially used to control the evaporator outlet temperature from deviating from set points. The control variable in this case is the pump speed. An increase in the pump speed will increase the mass flow rate of the working fluid which will cause a decrease in the evaporator outlet temperature (and vice-versa).

The PID parameters K_p , K_i , K_d and filter coefficient z were tuned in order to obtain a good compromise between the time requirement to achieve control stabilisation and a reduction of the control overshoot. The aim of the tuning process was to meet the requirement of having overshoot, rise time, and settling time equal to 3%, 18s, and 69s, respectively. The tuned values for the PID parameters are: $K_p = 84.07$, $K_i = 3.59$, $K_d = 72.69$ and $z = 0.138$.

The control performance and control signal of the PID controller for a step change are shown in Fig.7 and Fig. 8, respectively. At time 0 s, a step change of 3 K is applied to the initial set point temperature of 405 K. The response of the evaporator outlet temperature T_{ro} and the pump speed with respect to the step change are found to be satisfactory. It can be seen from Fig. 7 that the desired set point temperature can be achieved within 100s. To meet the set point demand, the controller changed the control signal swiftly as shown in Fig. 8

The response of T_{ro} and the performance of the controller are also tested to demonstrate the variable set points tracking ability when the system input condition changes. Fig. 9 presents the system response with respect to different input conditions as listed in Table 3. These cases are within the nominal heat inputs that can be used

for low and medium grade and micro-scale WHR systems [18,28].

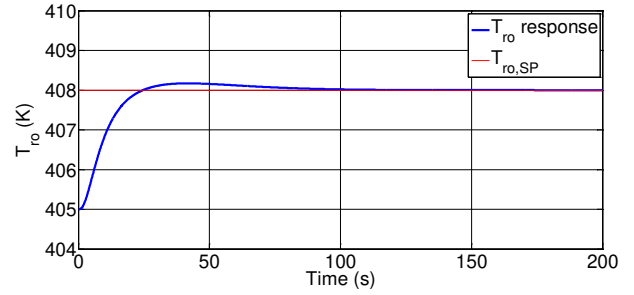


Fig. 7. Response of T_{ro} with a step change of $T_{ro,SP}$

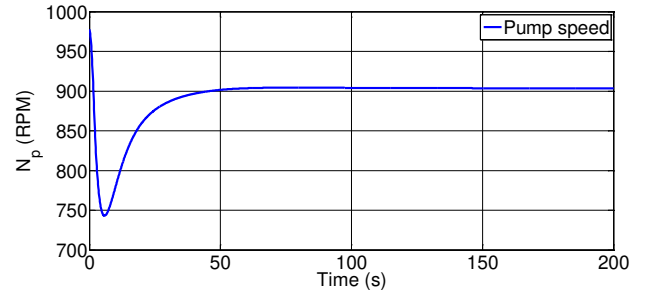


Fig. 8. Response of pump speed

Table 3. Nominal heat inputs to WHR system

Case	\dot{m}_h (kg/s)	T_h (K)
Case 1	0.2	500
Case 2	0.25	490
Case 3	0.22	485

Fig. 9 indicates that the tracking performance of the PID controller vary for different input conditions. Although the reference set points are kept the same for all cases, the performance of the controller for cases 2 and 3 are reduced significantly. Therefore, the design of a self-tuning PID controller and its performance in comparison with the conventional PID controller are discussed in the next section.

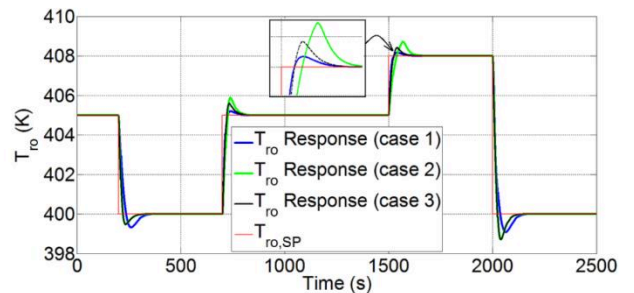


Fig. 9. Variable set point tracking of PID controller under different input conditions

4.2 Fuzzy self-tuning PID controller

The evaporator temperature is the critical parameter which is likely to be affected by the variable input conditions. Since the evaporator has a high thermal inertia and slow response, the conventional PID controller with invariable parameters is expected to work

inefficiently in the presence of transient disturbances. Therefore, a fuzzy self-tuning PID controller is proposed to improve the control performance in this research. The fuzzy self-tuning method provides an opportunity to adjust the PID parameters when a system is running with variable input conditions [29,30]. The structure of the fuzzy self-tuning PID controller is shown in Fig. 10(a).

The fuzzy self-tuning PID controller consists of two separate functional parts: the fuzzy tuner and the PID controller, as shown in Fig. 10. The fuzzy tuner has two inputs: the error $e(t)$ between the reference and measured value of the evaporator outlet temperature, and the rate of change of the error $de(t)$, and three outputs are the PID parameters K_p , K_i and K_d .

The inputs of the fuzzy tuner are defined by three subsets. They are SE: small error, ME: medium error and LE: large error for the $e(t)$; LR: Low rate, MR: medium rate and HR: high rate for the $de(t)$. The fuzzy subsets assigned to the output variables K_p and K_i are L: low, LM: low to medium, M: medium, MH: medium to high and H: High, and for the K_d are L: low, M: medium and H: high. The range of the inputs and outputs parameters are defined as follows: $e(t)_{[\min, \max]} = [-10, 10]$, $de(t)_{[\min, \max]} = [-100, 100]$, $K_{p[\min, \max]} = [80, 300]$, $K_{i[\min, \max]} = [1, 5]$ and $K_{d[\min, \max]} = [-300, 300]$. The membership functions of the inputs and the normalised outputs fuzzy subsets and their ranges are shown in Fig. 11. The inputs of the fuzzy tuner are obtained from an estimated range of error and its rate of change for the WHR system, while the outputs variable ranges are determined from the PID control simulation and adjusted according to the performance requirement.

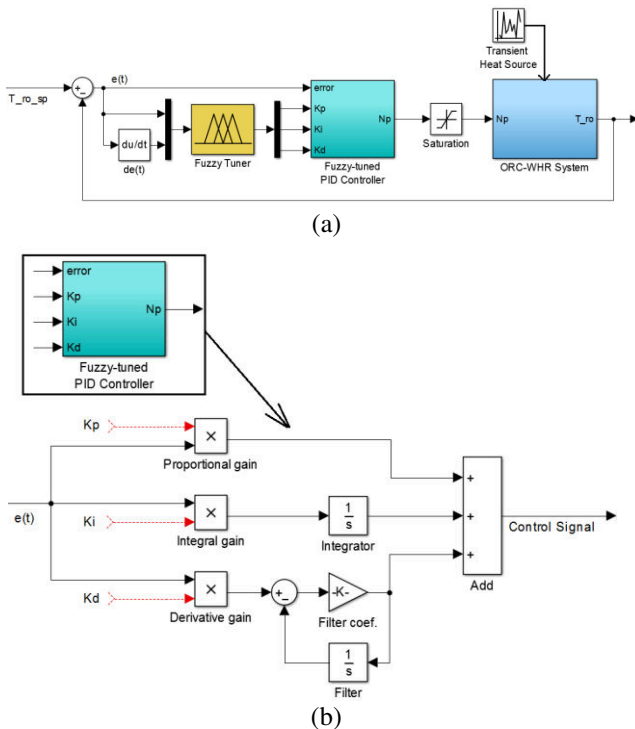


Fig. 10. (a) Structure of fuzzy self-tuning PID controller, (b) Inside structure of fuzzy-tuned PID controller

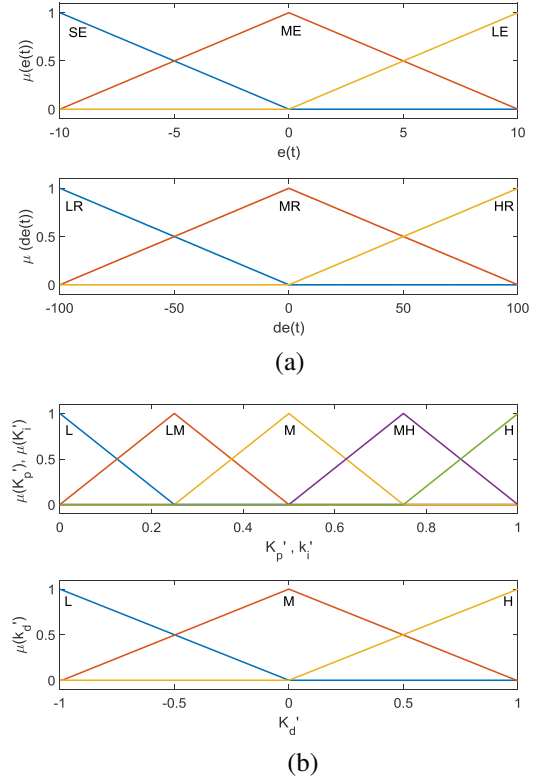


Fig. 11. Membership functions of (a) $e(t)$ and $de(t)$, (b) K_p , K_i and K_d [“'” represents normalised value]

The rules of the fuzzy tuner are created utilizing the fuzzy IF-THEN statements and with the mentioned fuzzy sets of the input and output variables, and can be presented as follows:

Rule l : IF $e(t)$ is α_j AND $de(t)$ is β_j THEN K'_p is δ_j AND K'_i is ϕ_j AND K'_d is λ_j (11)

where $j = 1, 2, 3, \dots, n$, n is the number of fuzzy rules which is nine in this case, α_j , β_j , δ_j , ϕ_j and λ_j are the j^{th} fuzzy sets of the input and output variables of the fuzzy system. The rules are established based on the dynamic characteristics of the ORC-WHR system, as detailed in [21,22] and simulations from the PID controller, which are shown in surfaces in Fig. 12.

For a given particular input fuzzy set α' in U , the output fuzzy set δ' in S for K'_p is computed through the MAX-Min fuzzy inference system as follows:

$$\mu'_{\delta'}(K'_p) = \max_{l=1}^n \left[\sup_{x \in U} \min \left\{ \mu_{\alpha'_l}(x), \mu_{\alpha'_l}(e(t)), \mu_{\beta'_l}(de(t)), \mu_{\delta'_l}(K'_p) \right\} \right] \quad (12)$$

Similarly, the output membership functions for K'_i and K'_d are calculated in (12). In this research, the membership functions used for the fuzzy tuner are triangular type, and their normalised form is denoted by μ' .

To convert the aggregated fuzzy set to a crisp output value Y from the fuzzy set δ' in $V \subset R$, the centroid defuzzification method is used in this model, which computes the centre of gravity of the membership function curves by (13).

$$Y = \frac{\int_V \mu_{\delta'}(y) \cdot y dy}{\int_V \mu_{\delta'}(y) dy} \quad (13)$$

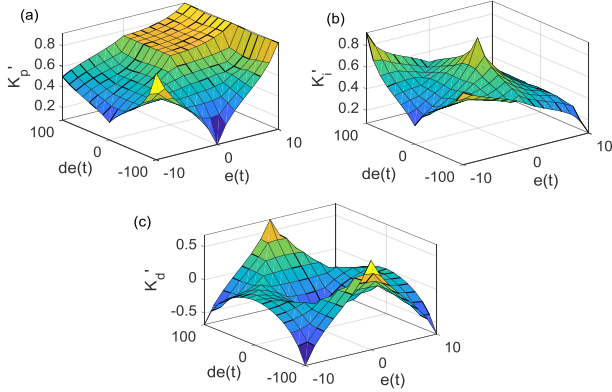


Fig. 12. Fuzzy control rules (a) K_p (b) K_i and (c) K_d

The performance of the fuzzy-self tuning PID controller tested for set point tracking and robustness and compared with the conventional PID controller is presented in the following sections.

4.2.1 Set point tracking for evaporator temperature

To investigate the set point tracking ability of the controllers, variable steps of the evaporator temperature are used as the reference inputs of the ORC-WHR system. The steps variations are selected as follows: at $t = 200$ s, $T_{ro,SP}$ drops from an initial value of 405 K to 402 K; at $t = 700$ s, the set point increases to 405 K; at $t = 1500$ s, the set point further rises to 407 K; and finally at $t = 2000$ s, the set point declines to 400 K. These step changes are arbitrarily chosen around the ideal temperature which is described in Section 3. During this test, the nominal input parameters to the system, $\dot{m}_h = 0.2$ kg/s and $T_h = 500$ K, are kept constant. The corresponding responses of the process variables, T_{ro} and W_{exp} , and the control input N_p are shown in Figs. 13-15.

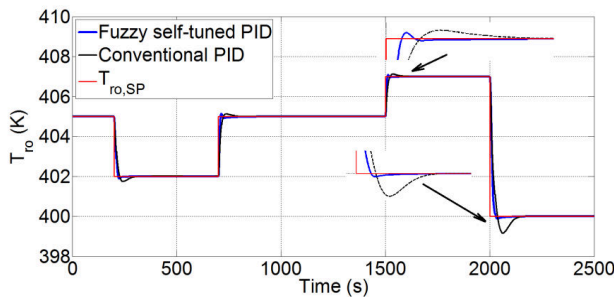


Fig. 13. Response of T_{ro} with respect to variable steps.

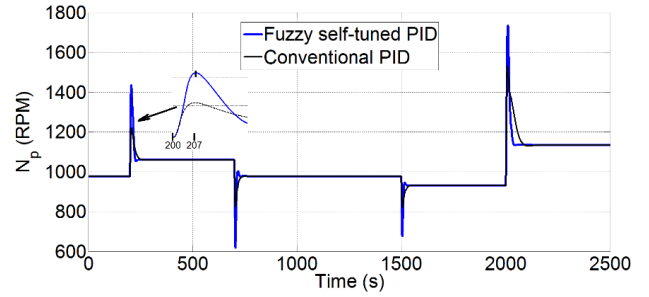


Fig. 14. Variation of pump speed

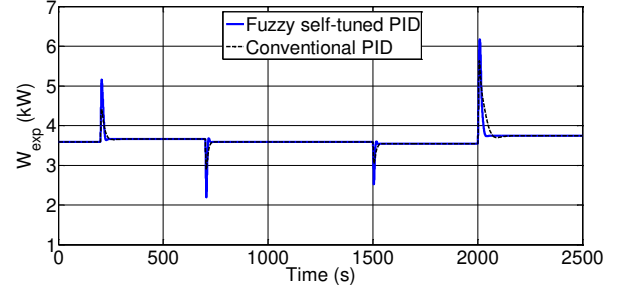


Fig. 15. Response of expander work output

Fig. 13 demonstrates that the response of T_{ro} for the fuzzy self-tuning PID controller is faster than that of the conventional PID controller. It also shows that the former controller achieves the temperature steadiness within a shorter time and reduces the system overshoot significantly. Fig. 14 shows that the control variable, pump speed, changes with respect to control demand at a rate less than 100 rpm/s, which is within the pump's specification and is desirable for pumps used in small-scale WHR systems [18]. Fig. 15 illustrates the response of the expander power output which is not controlled in this strategy. Therefore, the expander output is expected to vary with the pump speed (or the mass flow rate) since the power output is a function of the mass flow rate of the working fluid.

4.2.2 Robustness of fuzzy self-tuning PID controller

The robustness of the fuzzy self-tuning PID controller is examined and compared with the conventional PID controller in two scenarios: by investigating the control performance with respect to set point tracking under high-frequency heat sources and the heat sources with high-frequency white noises to the mass flow rate and temperature.

In the first scenario, the high-frequency heat source shown in Fig. 16 is applied to the ORC-WHR system. The controller performances are examined for its ability to track the variable steps set points. Figs. 17-18 represent the control performance with respect to step tracking. Fig. 17 shows that the fuzzy self-tuning PID controller has effectively adjusted the evaporator outlet temperature even when the set point values are changed. It can be seen from Fig. 18 that when the step changes occur, the controllers change the control signal greatly which reflects in the sudden changes in the pump speed.

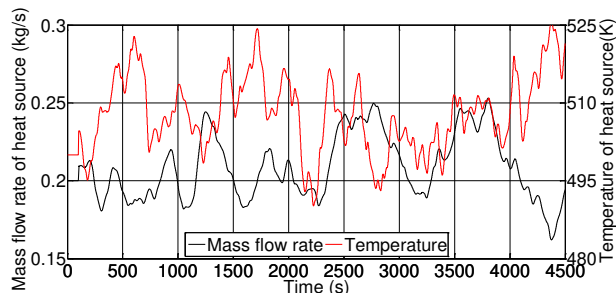


Fig. 16. Transient heat sources

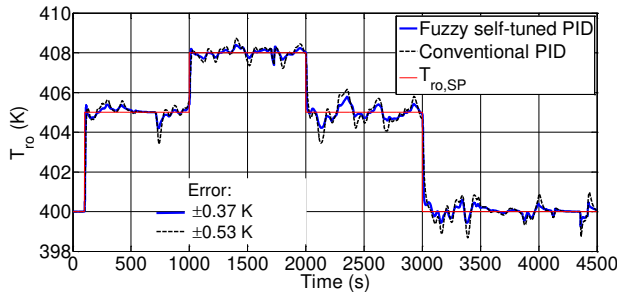


Fig. 17. Response of T_{ro} with respect to variable step set points

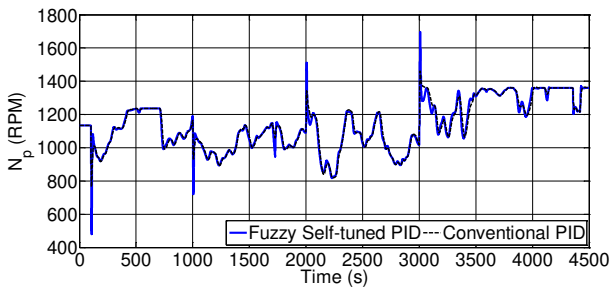


Fig. 18. Variation of pump speed

In reality, the measurement of the heat source flow rate and temperature from sensors is not smooth, instead, there is always some degree of noise. To imitate this situation, two white noises are added to the mass flow rate and temperature shown in Fig. 16. Therefore the heat source with the different frequency and amplitude noises used in the simulation is shown in Fig. 19.

The control performance of both controllers with the high transient noisy heat source is presented in Figs. 20-21. The response of the fuzzy self-tuning PID controller is within a range of ± 0.33 K against the set point demand, while it is found to be ± 0.58 K for the conventional PID controller. The control variable shown in Fig. 21 is adjusted according to the set point demand in Fig. 20.

In this simulation, the fuzzy self-tuning PID controller showed that the set point of the process variable can be tracked more accurately than the conventional PID controller despite abrupt fluctuations in the heat source inputs. Therefore, it is evident that the developed fuzzy self-tuning PID is a robust controller which can be used to control the evaporator temperature of the ORC-WHR system.

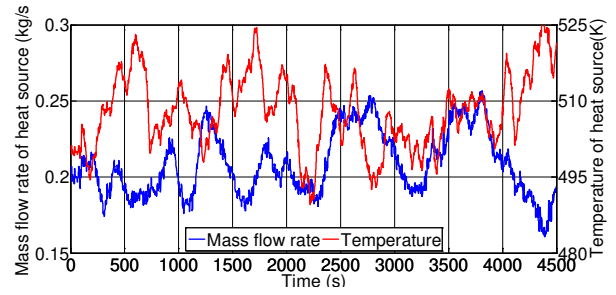


Fig. 19. Transient heat source with white noises

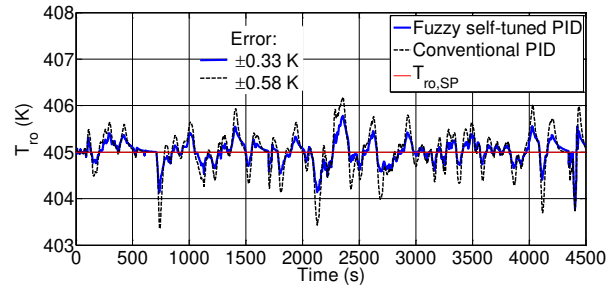


Fig. 20. Response of T_{ro} with respect to transient heat source

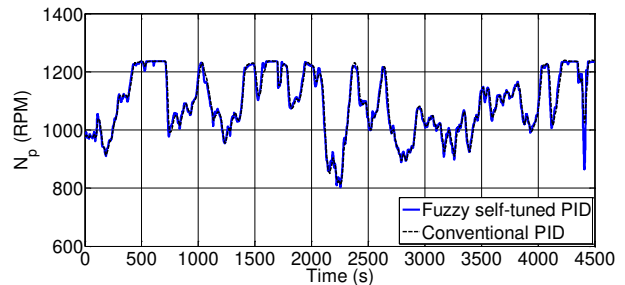


Fig. 21. Variation of pump speed

5. SIMULATION OF SIMULTANEOUS CONTROL OF EVAPORATOR TEMPERATURE AND EXPANDER OUTPUT

As described earlier, the sudden rise of the pump speed in the previous control strategy causes an almost instant rise of the expander work output which can be seen in Fig. 15. The second control strategy, which consists of the evaporator temperature and expander output control, in this section is therefore aimed at reducing the sudden rise of the expander work output and maintaining it at a desired set point. To achieve this, an independent Proportional-Integral (PI) controller is used to regulate the valve opening, which controls the expander work output. Note that the response of an expander in ORC-WHR systems is much faster than the response of an evaporator, as discussed earlier, and hence a simple PI controller is assumed to be sufficient for expander output control, which is also supported in [18]. The overall WHR control system using the second control strategy is therefore shown in Fig. 22. In this control system, both the fuzzy-self tuning PID and the PI controller are implemented simultaneously.

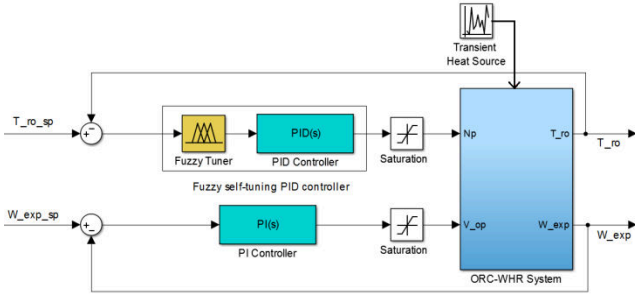


Fig. 22. Overall control structure of ORC-WHR system

The PI parameters were tuned using MATLAB Automatic PID Tuner with the aim of meeting the requirements of having 0% overshoot, 1.89 s rise time, and 3.2 s settling time. The tuned parameters for the PI controller are $K_p = 0.30$ and $K_i = 0.32$.

To simulate the performance of the two controllers in the combined control system at a dynamic condition, the transient heat source shown in Fig. 16 is imposed on the ORC-WHR system.

Fig. 23 shows that the process variable, evaporator outlet temperature, of the fuzzy self-tuning PID controller always follows the set point value despite the variation of the mass flow rate and temperature of the heat source in Fig. 16. However, because of the transient nature of the heat source, the process variable never reached the steady-state value, which was as expected and is similar to the results from the literature in [31]. However, in spite of 40 K variation in the heat source temperature, the maximum deviation of evaporation temperature from the set point value never exceeded 1 K.

Fig. 24 shows the expander power output when using two controllers; the dotted black line represents the expander output without the valve control, and the blue line represents the output with the valve control. It is clearly evident that without the valve control, the expander experiences heavy fluctuations during the simulation period. This fluctuation may not be a good operating condition for an expander in a small-scale waste heat recovery application. But with the valve control, the expander output remains almost steady around the set point except for some disturbances in certain times of the operation.

Figs. 25-26 demonstrate the change of the control signals within the operation period. It can be observed from Fig. 26 that the valve opening at certain times reaches its saturation value, i.e., it is fully open. Especially, at the time between $t = 2134$ s and $t = 2330$ s. This is because at these times the heat quantity in the heat source is low, but the temperature at the evaporator outlet has to maintain the set point value. In an attempt to match the set point temperature, the pump speed is reduced (see Fig. 25), which causes a decrease in the mass flow rate at the inlet of the valve. Since the mass flow rate is a function of the expander work output, the valve opens or closes according to the set point value. Because of the lower mass flow rate, the valve is fully opened to meet the expander output set value. After having a deviation from the set point, the PI controller regains the control and the work output gets returned to the set demand swiftly.

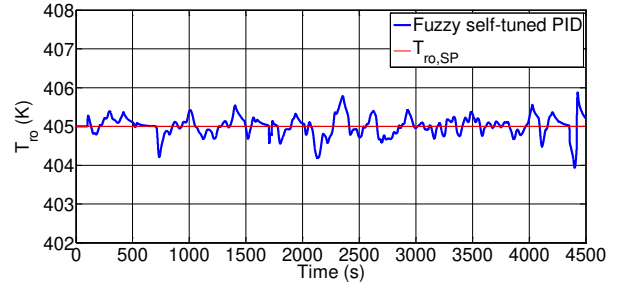


Fig. 23. Response of evaporator outlet temperature

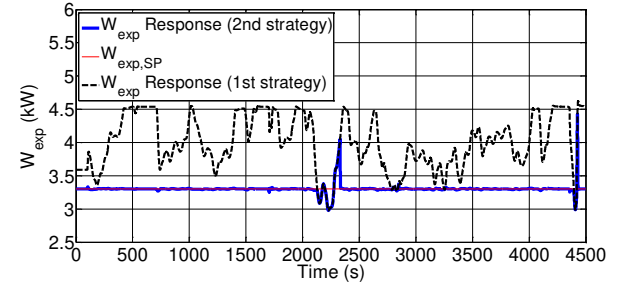


Fig. 24. Response of expander work output

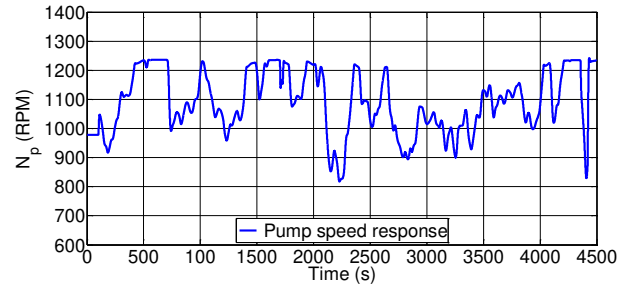


Fig. 25. Variation of pump speed

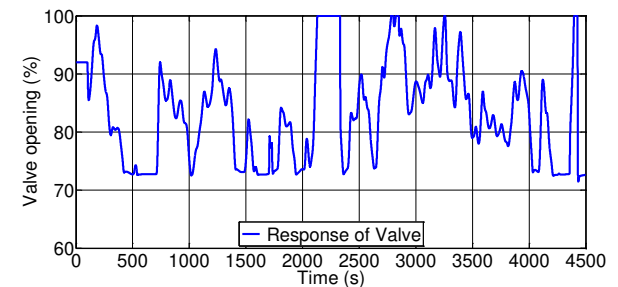


Fig. 26. Variation of valve opening

6. CONCLUSIONS

In this paper, the dynamic model of the ORC-WHR system was developed and presented. The dynamic model was then used to develop control strategies and control algorithms to simulate the control performance with respect to steady and transient heat input conditions.

Since the evaporator was the focus of the research, the dynamic model of this component was developed using the fuzzy inference system which reduces the computation time significantly. The proposed model of the evaporator was integrated with other components such as a pump, an expander, a condenser, an accumulator, and a modulating control valve to provide a complete overall model of the WHR system.

Since the operating parameters of the ORC-WHR system are influenced by the variable heat sources, two control strategies were proposed. The first control strategy was aimed at controlling the evaporator outlet temperature by regulating the pump speed, which was found to be critical in this research. To improve control performance, the PID parameters were adjusted in real time using the fuzzy inference system. The performance of the fuzzy self-tuning PID controller was compared with the conventional PID controller and results indicated that the fuzzy self-tuning PID controller improved the control performance significantly. This demonstrates that the developed fuzzy self-tuning PID controller is robust enough to handle the uncertain disturbances which are common in the WHR systems. The second control strategy, on the other hand, was aimed at controlling the expander power output by adjusting the valve opening. In this strategy, the expander output was controlled by an independent PI controller along with the fuzzy self-tuning PID controller which was used to control the evaporator outlet temperature. The second strategy provides a better control of the process variables of the ORC-WHR system.

Although the performance of the fuzzy self-tuning PID controller in set point tracking and disturbance rejection has improved significantly, the controller's capabilities will have to be explored in the context of start-up and shut-down procedures to ensure the safety of the ORC-WHR system, which is a task for future research.

REFERENCES

- [1] United States Environmental Protection Agency, "Global Greenhouse Gas Emissions Data," 2017. [Online]. Available: <https://www.epa.gov/ghgemissions/global-greenhouse-gas-emissions-data>. [Accessed: 01-Jun-2016].
- [2] J. I. Chowdhury, Y. Hu, I. Haltas, N. Balta-Ozkan, G. J. Matthew, and L. Varga, "Reducing industrial energy demand in the UK: A review of energy efficiency technologies and energy saving potential in selected sectors," *Renewable and Sustainable Energy Reviews*, vol. 94, pp. 1153–1178, 2018.
- [3] J. I. Chowdhury, B. K. Nguyen, and D. Thornhill, "Investigation of waste heat recovery system at supercritical conditions with vehicle drive cycles," *Journal of Mechanical Science and Technology*, vol. 31, no. 2, pp. 923–936, 2017.
- [4] A. Schuster, S. Karellas, and R. Aumann, "Efficiency optimization potential in supercritical Organic Rankine Cycles," *Energy*, vol. 35, no. 2, pp. 1033–1039, Feb. 2010.
- [5] X. Dai, L. Shi, Q. An, and W. Qian, "Screening of hydrocarbons as supercritical ORCs working fluids by thermal stability," *Energy Conversion and Management*, vol. 126, pp. 632–637, 2016.
- [6] E. Wang, Z. Yu, H. Zhang, and F. Yang, "A regenerative supercritical-subcritical dual-loop organic Rankine cycle system for energy recovery from the waste heat of internal combustion engines," *Applied Energy*, vol. 190, pp. 574–590, 2017.
- [7] J. I. Chowdhury, B. K. Nguyen, and D. Thornhill, "Modelling of Evaporator in Waste Heat Recovery System using Finite Volume Method and Fuzzy Technique," *Energies*, vol. 8, no. 12, pp. 14078–14097, 2015.
- [8] H. Singh and R. S. Mishra, "Performance evaluation of the supercritical organic rankine cycle (SORC) integrated with large scale solar parabolic trough collector (SPTC) system: An exergy energy analysis," *Environmental Progress and Sustainable Energy*, vol. 37, no. 2, pp. 891–899, 2018.
- [9] J. I. Chowdhury, P. Soulatiantork, and B. K. Nguyen, "Simulation of Waste Heat Recovery System with Fuzzy Based Evaporator Model," in *11th Asian Control Conference (ASCC)*, pp. 2143–2147, 2017.
- [10] B. Dong, G. Xu, X. Luo, L. Zhuang, and Y. Quan, "Analysis of the supercritical organic Rankine cycle and the radial turbine design for high temperature applications," *Applied Thermal Engineering*, vol. 123, pp. 1523–1530, 2017.
- [11] J. I. Chowdhury, B. K. Nguyen, D. Thornhill, R. Douglas, and S. Glover, "Modelling of Organic Rankine Cycle for Waste Heat Recovery Process in Supercritical Condition," *International Journal of Mechanical and Mechatronics Engineering*, vol. 9, no. 3, pp. 477–482, 2015.
- [12] J. Patiño, R. Llopis, D. Sánchez, C. Sanz-Kock, R. Cabello, and E. Torrella, "A comparative analysis of a CO₂ evaporator model using experimental heat transfer correlations and a flow pattern map," *International Journal of Heat and Mass Transfer*, vol. 71, pp. 361–375, 2014.
- [13] J. Sun and W. Li, "Operation optimization of an organic rankine cycle (ORC) heat recovery power plant," *Applied Thermal Engineering*, vol. 31, no. 11–12, pp. 2032–2041, 2011.
- [14] J. I. Chowdhury, B. K. Nguyen, and D. Thornhill, "Fuzzy based evaporator model in waste heat recovery system," in *3rd International Conference on Fluid Flow, Heat and Mass Transfer (FFHMT'16)*, 2016.
- [15] J. Zhang, K. Li, and J. Xu, "Recent developments of control strategies for organic Rankine cycle (ORC) systems," *Trans. of the Institute of Measurement and Control*, 2018.
- [16] J. Zhang, Y. Zhou, Y. Li, G. Hou, and F. Fang, "Generalized predictive control applied in waste heat recovery power plants," *Applied Energy*, vol. 102, pp. 320–326, 2013.
- [17] A. Yebi, B. Xu, X. Liu, J. Shetty, P. Ansel, S. Onori, Z. Filipi, and M. Hoffman, "Nonlinear Model Predictive Control Strategies for a Parallel Evaporator Diesel Engine Waste Heat Recovery System," in *Proceedings of the ASME 2016 Dynamic Systems and Control Conference*, pp. 1–9, 2016.
- [18] S. Quoilin, R. Aumann, A. Grill, A. Schuster, V. Lemort, and H. Spliethoff, "Dynamic modeling and optimal control strategy of waste heat recovery Organic Rankine Cycles," *Applied Energy*, vol. 88,

no. 6, pp. 2183–2190, 2011.

- [19] X. Zhao, P. Shi, and X. Zheng, “Fuzzy Adaptive Control Design and Discretization for a Class of Nonlinear Uncertain Systems,” *IEEE Trans. on Cybernetics*, vol. 46, no. 6, pp. 1476–1483, 2016.
- [20] H. Wang, P. X. Liu, and B. Niu, “Robust Fuzzy Adaptive Tracking Control for Nonaffine Stochastic Nonlinear Switching Systems,” *IEEE Trans. on Cybernetics*, vol. 48, no. 8, pp. 2462–2471, 2018.
- [21] J. I. Chowdhury, B. K. Nguyen, and D. Thornhill, “Dynamic model of supercritical Organic Rankine Cycle waste heat recovery system for internal combustion engine,” *International Journal of Automotive Technology*, vol. 18, no. 4, pp. 589–601, Aug. 2017.
- [22] J. I. Chowdhury, B. K. Nguyen, D. Thornhill, Y. Hu, P. Soulatiantork, N. Balta-Ozkan, and L. Varga, “Fuzzy Nonlinear Dynamic Evaporator Model in Supercritical Organic Rankine Cycle Waste Heat Recovery Systems,” *Energies*, vol. 11, no. 4, p. 901, 2018.
- [23] Y. Wei, J. Qiu, and H. R. Karimi, “Fuzzy-Affine-Model-Based Memory Filter Design of Nonlinear Systems with Time-Varying Delay,” *IEEE Trans. on Fuzzy Systems*, vol. 26, no. 2, pp. 504–517, 2018.
- [24] Y. Wei, J. Qiu, and H. K. Lam, “A Novel Approach to Reliable Output Feedback Control of Fuzzy-Affine Systems with Time Delays and Sensor Faults,” *IEEE Trans. on Fuzzy Systems*, vol. 25, no. 6, pp. 1808–1823, 2017.
- [25] Hydra-Cell, “Installation and service manual: Hydra-Cell Industrial pumps.” [Online]. Available: <http://www.hydra-cell.com/product/D03-hydracell-pump.html>. [Accessed: 01-May-2015].
- [26] S. E. Haaland, “Simple and Explicit Formulas for the Friction Factor in Turbulent Pipe Flow,” *Journal of Fluids Engineering*, vol. 105, no. 1, pp. 89–90, 1983.
- [27] J. I. Chowdhury, “Modelling and Control of Waste Heat Recovery System,” Queens University Belfast, 2017.
- [28] S. Quoilin, “Sustainable energy conversion through the use of Organic Rankine Cycles for waste heat recovery and solar applications,” University of Liège, 2011.
- [29] A. Fadaei and K. Salahshoor, “A novel real-time fuzzy adaptive auto-tuning scheme for cascade PID controllers,” *International Journal of Control Automation and Systems*, vol. 9, no. 5, pp. 823–833, 2011.
- [30] S. Barghandan, M. A. Badamchizadeh, and M. R. Jahed-motlagh, “Improved Adaptive Fuzzy Sliding Mode Controller for Robust Fault Tolerant of a Quadrotor,” *International Journal of Control Automation and Systems*, vol. 15, no. 1, pp. 427–441, 2017.
- [31] M. C. Esposito, N. Pompini, A. Gambarotta, V. Chandrasekaran, J. Zhou, and M. Canova, “Nonlinear model predictive control of an Organic Rankine Cycle for exhaust waste heat recovery in automotive engines,” *IFAC-PapersOnLine*, vol. 28,

no. 15, pp. 411–418, 2015.



Jahedul Islam Chowdhury received the PhD in Mechanical Engineering from Queens University Belfast, UK in 2017. His research interests include low carbon heat, waste heat to energy conversion technologies, energy efficiency, renewable energy sources, modelling and control of nonlinear energy systems, and conventional and intelligent control.



David Thornhill received PhD in Mechanical Engineering from Queen’s University Belfast, UK in 1988. Since 1995 he has been an academic in the School of Mechanical & Aerospace Engineering at Queen’s University Belfast specializing in energy conserving research projects



Payam Soulatiantork received the PhD in Electrical Engineering from Polytechnic of Milan, Italy in 2016. His research interests include nonlinear control, SCADA system, adaptive control, industrial automation, real time control and monitoring.



Yukun Hu received the PhD in Chemical Engineering from Royal Institute of Technology, Sweden, in 2013. His research interests include Energy process simulation, analysis, optimisation and control.



Nazmiye Balta-Ozkan received the PhD in Regional Planning with specialisation on Environmental Economics from University of Illinois at Urbana-Champaign, USA in 2004. Her research interests include energy and environment, energy economics, energy policy and environmental impacts.



Liz Varga received the PhD from Cranfield University, UK 2009. Her research interests include trans-disciplinary infrastructure systems (energy, transport, water, waste and telecoms), agent based models, dynamics of interconnected systems, modelling the effects of policy, technology and innovation under different scenarios.



Bao Kha Nguyen Received the PhD in Mechatronics from University of Ulsan, South Korea in 2007. His research interests include control systems, industrial automation, mechatronics, robotics, smart sensors and actuators, design and implementation of real time control systems for industrial applications using intelligent and advanced control algorithms.